Ab initio study of long-period superstructures in close-packed A3B compounds

Rosengaard, N. M.; Skriver, Hans Lomholt

Published in:
Physical Review B

Link to article, DOI:
10.1103/PhysRevB.49.14666

Publication date:
1994

Document Version
Publisher's PDF, also known as Version of record

Ab initio study of long-period superstructures in close-packed A_3B compounds

N. M. Rosengaard and H. L. Skriver
Center for Atomic-Scale Materials Physics and Physics Department, Technical University of Denmark, DK-2800 Lyngby, Denmark
(Received 16 November 1993)

We have performed *ab initio* calculations of the stability of one-dimensional long-period superstructures in Cu_3Pd, Cu_3Al, and Ag_3Mg by means of an interface Green's function technique based on the linear-muffin-tin-orbitals method within the tight-binding and atomic-sphere approximations. The energies of the superstructures relative to the $L1_2$ structure are found by an expansion based on the calculated energy of a single (001) antiphase boundary and the calculated interaction energy between two and three antiphase boundaries of varying distance. The expansion agrees with standard band-structure calculations of the structural energy differences for the two short-period superstructures DO_{22} and DO_{23}. We find that at zero temperature the ground states of Cu_3Pd, Cu_3Al, and Ag_3Mg are one-dimensional superstructures with antiphase boundary separations of 2–5 unit cells of the underlying $L1_2$ structure.

I. INTRODUCTION

In a number of ordered face-centered-cubic (fcc) A_3B compounds one observes experimentally[1–15] so-called one-dimensional long-period superstructures (1D-LPS's) which are lattices based on the $L1_2$ structure and which may be viewed as periodic arrangements of (001) antiphase boundaries (APB's) of the kind shown in Fig. 1. From a theoretical point of view such a periodic arrangement may be stable at low temperature if the energy of a single antiphase boundary is negative, and in that case the period of the superstructure will be determined by a competition between the energy gained in the formation of densely spaced antiphase boundaries and the large repulsion between neighboring antiphase boundaries which are brought close together.

The formation of long-period superstructures may be studied by means of standard one-electron methods employing a supercell approach. However, for structures with an antiphase boundary separation M larger than 3 unit cells of the underlying $L1_2$ structure the supercells become formidably large and to our knowledge there exist *ab initio* calculations only for selected compounds in the two simplest stuctures, DO_{22} and DO_{23}.[16,17] To circumvent this problem we start from the antiphase boundary energies calculated by Rosengaard and Skriver[18] and add the repulsion between two and three antiphase boundaries obtained as a function of separation by means of our interface Green's function technique.[19,20] This approach has the advantage that the computational effort scales linearly with the number of layers and hence we are able to treat superstructures with M up to at least 19 $L1_2$ unit cells.

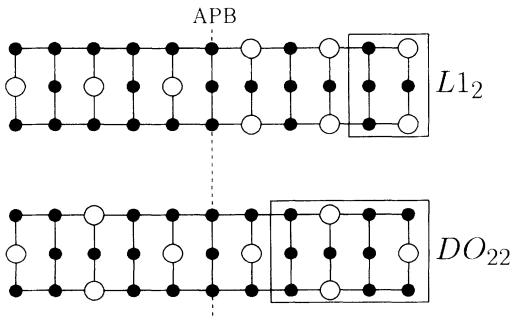

FIG. 1. Schematic representation of (001) antiphase boundaries in (a) the $L1_2$ and (b) the DO_{22} crystal structures. The filled (open) circles represent the majority (minority) atoms. Stacking in [001] direction alternates between pure layers, consisting of only majority atoms, and mixed layers consisting of a centered square lattice plane of majority and minority atoms.

Here we present results for three ordered intermetallic compounds Cu_3Pd, Cu_3Al, and Ag_3Mg which we found to have negative antiphase boundary energies in the $L1_2$ stucture[18] and which experimentally are found to exhibit long-period superstructures. In our approach the period of a superstructure is found from the antiphase boundary separation which minimizes the total energy and which corresponds to the electronic ground state of the system at low temperature. Thus we exclude the effect of entropy. However, the results may be used as the basis for model Hamiltonians and statistical mechanics simulations.

A. Experimental

The Cu_3Pd system is well studied experimentally both by x-ray diffraction[1,2] and more recently by high resolution electron microscopy (HREM).[3,4] In the HREM study of Broddin *et al.*[3] the annealing temperatures were between 200 °C and 440 °C, and at a Pd concentration

of 24.5% these authors found a mean antiphase boundary separation of $M = 4.5$, consistent with a separation alternating between 4 and 5 unit cells of the underlying $L1_2$ structure. Furthermore, the antiphase boundary separation decreased with increasing Pd concentration and at 30% the 1D-LPS consisted of a sharp periodic antiphase domain structure with a separation of $M = 3$. In a similar study, Takeda *et al.*[4] reported a long-period superstructure with an antiphase boundary separation of $M = 4$ at a Pd concentration of 25.2% and for annealing temperatures between 350 °C and 500 °C. In addition, antiphase boundary separations between 3 and 4 were observed above 25% Pd. Neither Broddin *et al.*[3] nor Takeda *et al.*[4] observed any temperature dependence for Pd concentrations larger than approximately 22% but, at lower concentrations, the density of antiphase boundaries is observed to decrease at decreasing temperature. Below Pd concentrations of $\sim 20\%$, the $L1_2$ structure is observed.

Cu_3Al is observed in a 1D-LPS,[5–8] which may be described as an antiphase domain structure based on the DO_{22} crystal structure. The HREM study of Kuwano *et al.*[7] shows the antiphase boundary structure of Cu_3Al to consist of sharp and well defined commensurate structures in the concentration range 22–24 % Al. At 24% Al the spacing between antiphase boundaries in the DO_{22} structure M' is found to be ~ 5 unit cells of the underlying $L1_2$ structure. In the concentration range 22.3–24.2 % Broddin *et al.* find a number of stable structures with spacings between 4 and 5.

Ag_3Mg has been investigated by x-ray electron diffraction[9–11] as well as by HREM[12–15] and shows sharp commensurate structures. Near the stoichiometric composition Ag_3Mg is observed to form a 1D-LPS based on the DO_{23} structure that in itself may be regarded as a 1D-LPS with an antiphase boundary separation $M = 2$. The simplest 1D-LPS's observed in Ag_3Mg consist of a number of antiphase domains of length $M = 2$ terminated by a domain of length $M = 1$. In the notation of Fisher and Selke[26] commonly used in the description of 1D-LPS's, the DO_{23} structure is described as $\langle 2 \rangle$, whereas the 1D-LPS's in Ag_3Mg are described by $\langle 2^j 1 \rangle$, j integer. At higher temperatures longer and more complicated structures described by $\langle 2^i 1 2^j 1 \rangle$ where i and j are integers occur.[13]

B. Theoretical

The first explanation of the formation of long-period superstructures in terms of the electronic structure was provided by Sato and Toth,[21] who related the formation of LPS's to sheets of the Fermi surface at the Brillouin zone boundaries of the LPS. Recent theoretical work based on the Korninga-Kohn-Rostoker coherent potential approximation (KKR-CPA) also focuses on Fermi surface effects. Györffy *et al.*[22] find the effective pair interactions for $Cu_{1-c}Pd_c$ using the method proposed by Györffy and Stocks.[23] The Fourier transform of the effective pair interaction displays a minimum along the XW segment, a feature caused by the parallel sheets of Fermi surface calculated for $Cu_{1-c}Pd_c$ in the random state.[23] In their description, it is this minimum which causes the stability of the 1D-LPS. From the KKR-CPA effective pair interactions and Bragg-Williams mean field theory, Ceder *et al.*[24,25] determine the phase diagram of $Cu_{1-c}Pd_c$. In particular, they find the existence of 1D-LPS's for Pd concentrations exceeding 18%. Furthermore, in the range of Pd concentrations from 24% to 34% the period of the calculated 1D-LPS is in complete agreement with those observed in the HREM experiments[3,4] above 200 °C. In the KKR-CPA mean field phase diagram the 1D-LPS's observed at room temperature persist to 0 K and the experimentally observed temperature dependence of the mean antiphase boundary separation for samples of $\lesssim 22$ at. % Pd is not found.

Recently, Jordan *et al.*[17] calculated the relative stabilities of the $L1_2$, DO_{22}, and DO_{23} structures in Ag_3Mg. They found that among these three structures the DO_{23} was the most stable and suggested that the stability was due to a particular flat section of the Fermi surface in the $L1_2$ structure. They proceeded to identify the concentration dependence of the dimension of this section of Fermi surface with the series of long-period superstructures observed experimentally and thereby provided strong evidence for the picture that the formation of superstructures is driven by the topology of the Fermi surface.

From the statistical mechanics point of view, the phase diagram of the axial next-nearest-neighbor Ising (ANNNI) model is known from the low temperature expansion of Fisher and Selke[26] to contain long-period superstructures. It was therefore suggested[26–29] to describe the phase diagram of intermetallics displaying 1D-LPS's by the ANNNI model or by a generalization including more distant neighbor interactions. However, because of the shortage of electronic-structure calculations for these alloy systems the parameters of the model Hamiltonian had to be estimated from other sources. Thus, Kulik *et al.*[13] estimated the interaction parameters of a generalized ANNNI model for Ag_3Mg from x-ray scattering experiments on the disordered alloy,[30] while Ceder *et al.*[24,25] extracted the ground state of the $Cu_{1-c}Pd_c$ system from the phase diagram calculated in the mean field approximation. On the other hand, at the stoichiometric composition the ground state is directly accessible to electronic-structure calculations, and it is the aim of the present work to provide *ab initio* calculations of the ground state of the three most studied alloy systems exhibiting long-period superstructures.

II. COMPUTATIONAL METHOD

We have used our interface Green's function technique[19,20] based on the linear-muffin-tin-orbitals (LMTO) method within the atomic-sphere approximation (ASA) developed by Andersen and co-workers[31–37] to calculate the energy of (001) antiphase boundaries in the $L1_2$, DO_{22}, and DO_{23} crystal structures. In the original implementation the Green's function of an interface was found from the ground state of the perfect

crystal by a one-dimensional k-space integration. This technique proved to be rather time consuming for large systems, and to facilitate the present study, which includes self-consistent calculations for systems of more than 100 atoms, we have now adopted the principal-layer technique implemented within the LMTO-ASA framework by Kudrnovsky *et al.*[38] in connection with the coherent potential approximation for surfaces of disordered alloys. This technique is particularly efficient for interfaces with a large number of atomic layers, because the computational effort scales linearly with the number of so-called principal layers, as opposed to the cubic scaling of conventional approaches. A precise description of the implementation is given by Rosengaard and Skriver[18] in connection with the calculation of antiphase boundary energies.

Details of the calculations

At the outset of an antiphase boundary calculation, one needs starting potentials as well as total energies corresponding to the perfect, infinite crystal of the ordered alloy in which the antiphase boundary is to be embedded. To obtain this input, we perform self-consistent bulk calculations by means of the second order LMTO Hamiltonian, and calculate the one-electron contribution to the kinetic energy by integrating the bulk Green's function on a complex energy contour. The contour is chosen as a semicircle and the integration performed by a Gaussian technique on a mesh of 16 points distributed exponentially so as to increase the sampling density near the Fermi level. Furthermore, although it is more time consuming, we use in the bulk calculations a Brillouin zone based on the 2D zone of the antiphase boundary structure, and in the direction perpendicular to the plane of the 2D zone we use 400, 200, and 100 $\mathbf{k}_\perp$ points for the $L1_2$, DO_{22}, and DO_{23} structures, respectively. These large numbers are necessary because the Green's function for the antiphase boundary is calculated by the principal-layer technique, and hence is completely converged in terms of $\mathbf{k}_\perp$.

In the case of an ordered compound, one should ideally choose the radii of the atomic spheres so as to minimize the errors of the ASA. The ASA introduces two kinds of errors. The first kind is related to the shape approximation inherent in the use of atomic spheres. For fcc based compounds this kind of error may be minimized by choosing spheres of equal radii in which case the neglected interstitial regions of space and the size of the overlap between neighboring spheres are reduced to a minimum. The second kind of error is caused by describing the one-electron potential only within overlapping atomic spheres. The choice of equal sphere radii in a compound causes a discontinuity between the one-electron potentials at the surfaces of neighboring atomic spheres. This discontinuity may be large, especially if the Wigner-Seitz radii of the elemental metals deviate appreciably. In the present bulk and interface calculations we have minimized the discontinuity by choosing the relative radii as close as possible to the ratio of the radii of the elemental metals without increasing the overlap region too much. This is in the spirit of the guidelines given by Andersen[39] which aims at the best possible (spherically symmetric) description of the potential inside overlapping spheres.

Based on convergence tests the interface region which contains a single antiphase boundary and which is treated self-consistently consists of 31 atomic layers each holding two atoms. Thus, there are eight mixed and seven pure layers between the left-hand semi-infinite bulk crystal and the antiphase boundary, and eight mixed and seven pure layers between the antiphase boundary and right-hand semi-infinite bulk crystal. The geometry used to calculate the interaction between antiphase boundaries is obtained by introducing two or three antiphase boundaries separated by the appropriate number of layers at the position of the single antiphase boundary. These calculations are performed for separations of up to 19 $L1_2$ lattice parameters in the $L1_2$ structure and 12 $L1_2$ lattice parameters in the DO_{22} structure, totaling 148 and 112 atoms in the two structures, respectively.

The $\mathbf{k}_{||}$ integration is performed by means of 36 special points[40] in the irreducible part of the two-dimensional square Brillouin zone. Furthermore, to maintain charge neutrality the small excess charge ($< 10^{-4}$ electrons) of the antiphase boundary region is placed at two sheets just outside the fault structure, and the corresponding contribution to the one-electron potential and the total energy included. In this manner, we take approximate account of the charge connected with the Friedel oscillations and ensure fast convergence of the antiphase boundary energies in terms of the region size. Finally, for exchange and correlation we use the local density functional of Ceperley and Alder[41] as parametrized by Perdew and Zunger.[42]

III. GEOMETRY OF THE ONE-DIMENSIONAL SUPERSTRUCTURES

Viewed along the cube axis, the series of structures $L1_2$, DO_{22}, DO_{23}, and subsequent one-dimensional long-period superstructures may all be described as an alternate stacking of pure layers containing only majority atoms and mixed layers containing an equal number of minority and majority atoms. The mixed layers form a centered square lattice, in which the minority atoms occupy the center and the majority atoms the corners or vice versa. As a result the minority atoms are never nearest neighbors, and it is only their relative positions in subsequent mixed layers which distinguish the structures. It follows that the long-period superstructures are degenerate in energy if only nearest-neighbor effective pair potentials are used to describe their structural stability. To underline this feature of the $L1_2$, DO_{22}, DO_{23}, and long-period superstructures, they are often referred to as polytypes in fcc based A_3B compounds.

In the stacking sequences of pure and mixed lattice planes which describe the long-period superstructures two relative positions between subsequent mixed layers are possible. Either the translation [001] connects minority atoms in subsequent mixed layers or it connects minority atoms to majority atoms. The former case is the

stacking of the $L1_2$ structure while the latter is the stacking of the DO_{22} structure. The (001) antiphase boundary in the $L1_2$ structure shown in Fig. 1(a) is the plane boundary between crystallographic domains ordered according to the $L1_2$ structure but connected by stacking according to the DO_{22} structure across the plane of the antiphase boundary. In the same way the (001) antiphase boundary in the DO_{22} structure shown in Fig. 1(b) may be described as the plane boundary between two regions of stacking according to DO_{22} connected by stacking according to $L1_2$.

A long-period superstructure in fcc based A_3B compounds may be viewed as a periodic arrangement of antiphase boundaries, and its period is commonly given by the separation M of the antiphase boundaries measured in terms of the (001) lattice parameter of the underlying $L1_2$ structure. In fact both the DO_{22} and the DO_{23} structures may be described in this way by $M = 1$ and 2, respectively. However, in some cases such as the long-period superstructures based on the DO_{22} structure it is more convenient to give the period of the superstructure in terms of the size M' of the DO_{22} antiphase domain still measured in units of the underlying $L1_2$ structure. The connection between the two is $M = \frac{M'}{M'-1}$.

IV. STABILITY OF THE ONE-DIMENSIONAL SUPERSTRUCTURES

The energy E_{APB} of a single (001) antiphase boundary embedded in an infinite crystal of the $L1_2$ structure is a measure of the stability of this structure relative to the formation of a one-dimensional long-period superstructure. If E_{APB} is negative the $L1_2$ structure is unstable and the period of the superstructure is determined by a competition between the formation of densely spaced antiphase boundaries and the large repulsion between antiphase boundaries which are brought closely together. In a study of the (001) antiphase boundary in a series of intermetallics[18] the three compounds Cu_3Pd, Cu_3Al, and Ag_3Mg were found to have negative antiphase boundary energies in the $L1_2$ structure. Thus, the values reproduced in Table I represent the gain in energy per antiphase boundary in the three compounds which must be offset by repulsive terms to form a stable superstructure. These repulsive terms may in turn be found by interface Green's function calculations of the energy of interfaces containing two or three antiphase boundaries of varying separations whereby one finally may etablish the period of the superstructures in Cu_3Pd, Cu_3Al, and Ag_3Mg.

The two-body interaction I_n between neighboring antiphase boundaries is calculated as the energy of an infinite system containing two antiphase boundaries at a separation n from which one subtracts the energy of formation $2E_{\mathrm{APB}}$ of two antiphase boundaries at infinite separation. An example of such a structure with $n = M = 2$ is shown in Fig. 2. In a similar fashion, the three-body interaction $K_{n,m}$ may be calculated as the energy of a system containing three antiphase boundaries of separation n and m from which one subtracts $3E_{\mathrm{APB}}$ as well as the pairwise interaction energy $I_n + I_m$ between nearest-neighbor antiphase boundaries.

The definition of the three-body interaction adopted above corresponds to an expansion in terms of the range of interaction between antiphase boundaries. As an example, consider calculating the structural energy of the one-dimensional long-range superstructure defined by an antiphase boundary separation $M = 3$. In this case, the first contribution to the interaction energy is given by the two-body term I_3 which carries all information corresponding to an interaction range of 3. The next contribution is the three-body term $K_{3,3}$ which carries all information corresponding to an interaction range of 6 including the next-nearest two-body term I_6. One may continue to consider the four-body term corresponding to an interaction range of 9 but this and the following terms will be small and may be neglected. As it turns out in the calculations to be presented below, already the three-body term $K_{n,m}$ is small at the separations corresponding to the ground state superstructures and the expansion may therefore safely be terminated at the three-body term. As a result one arrives at a local picture where the interaction between successive antiphase boundaries is dominated by the pair interaction between nearest-neighbor antiphase boundaries.

A. APB Hamiltonian

In the present description the energy of a given antiphase domain structure consists of the energy gained by forming the antiphase boundaries and the repulsion

TABLE I. Atomic Wigner-Seitz radii S_{WS} and calculated (001) antiphase boundary energy per surface cell E_{APB} for Cu_3Pd, Cu_3Al, and Ag_3Mg in the $L1_2$ structure. Also listed is the antiphase boundary energy for Cu_3Al in the DO_{22} structure as well as the energy of a single antiphase domain of length $M = 1$ for Ag_3Mg in the DO_{23} structure.

	S_{WS} (Bohr)		E_{APB} (mRy)		$E_{M=1}$ (mRy)
Compound	Theory	Exp.[a]	$L1_2$	DO_{22}.	DO_{23}
Cu_3Pd	2.726[b]	2.713	-3.46		
Cu_3Al	2.687[c]	2.710	-4.13	-3.44	
Ag_3Mg	3.023[d]	3.036	-6.94		1.69

[a]See Ref. 44.
[b]$L1_2$.
[c]DO_{22}.
[d]DO_{23}

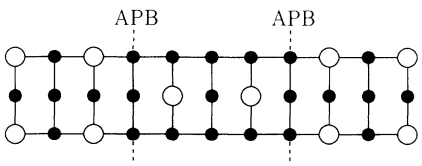

FIG. 2. Interface in the $L1_2$ crystal structure containing two antiphase boundaries at a distance $M = 2$. The pair interaction between nearest-neighbor APB's is calculated from the energy of this kind of structure as explained in the text. Notation as in Fig. 1.

between nearest-neighbor antiphase boundaries. This description may be mapped onto a one-dimensional effective Ising-like Hamiltonian in a field. To do so, we represent the presence of an antiphase boundary by $\uparrow$, $(S = \frac{1}{2})$ while the absence is represented by $\downarrow$, $(S = -\frac{1}{2})$, and the field is given by the energy E_{APB}. The interactions between neighboring antiphase boundaries are given by I_n and $K_{n,m}$ for two- and three-body interactions, respectively. As a result, the ground state energy for a given polytype may be found as

$$E = \sum_i [(S_i + \tfrac{1}{2})E_{\mathrm{APB}} + \sum_{j>i}{}' I_{j-i}(S_i + \tfrac{1}{2})(S_j + \tfrac{1}{2}) + \sum_{j>i>k}{}' K_{i-k,j-i}(S_i + \tfrac{1}{2})(S_j + \tfrac{1}{2})(S_k + \tfrac{1}{2})], \quad (1)$$

where the primes indicate that the sums are confined to nearest-neighbor $\uparrow$ spins. The Hamiltonian which is obtained by excluding the three-body terms and including all pair interactions was used by Bak and Bruinsma to study the complete devil's staircase.[43]

B. ANNNI Hamiltonian

One may arrive at a different expansion of the energy of a given antiphase domain structure if one applies a generalized ANNNI model to the problem of structural stability of the various 1D-LPS's. In the ground state of this model the atoms in each mixed layer are completely ordered. One need therefore only consider a one-dimensional Hamiltonian and may assign a single spin ($|\ S\ | = 1$) to each layer, the sign of which depends on which of the two inequivalent crystallographic positions is occupied by a minority atom. With these simplifications the ANNNI Hamiltonian becomes

$$H = -\sum_i \sum_{n\geq 1} J_n S_i S_{i+n}, \quad (2)$$

where the interaction parameters J_n which enter may be written

$$J_n = -\frac{1}{4} \times \begin{cases} I_2 - 2I_1 - 2E_{\mathrm{APB}}, & n = 1\ , \\ I_{n+1} - 2I_n + I_{n-1}, & n \geq 2\ , \end{cases} \quad (3)$$

in terms of the energy of formation E_{APB} of a single antiphase boundary and the interaction I_n between two isolated antiphase boundaries as calculated by the interface Green's function technique. It is seen that the J_n parameters are proportional to the curvature of the calculated interaction I_n viewed as a function of the antiphase boundary separation n. One should note that (3) is written specifically for an expansion based on antiphase boundaries in the $L1_2$ structure and that the right-hand side should be multiplied by $(-1)^n$ if the interactions I_n are calculated from antiphase boundaries within the DO_{22} structure.

V. BAND CALCULATIONS OF STRUCTURAL STABILITY

The DO_{22} and DO_{23} structures are one-dimensional superstructures the sizes of which are sufficiently small to allow calculations of their stability by means of standard band-structure methods. In Table II we compare the present results with available *ab initio* calculations and we note that although the absolute values differ considerably the relative stabilities agree. For Cu_3Pd in the DO_{22} structure at least part of the 40% deviation may be attributed to the fact that Lu *et al.*[16] used the linear augmented plane wave (LAPW) method and Wigner exchange correlation. On the other hand, it is difficult to reconcile the two sets of LMTO-ASA band-structure calulations for Ag_3Mg, especially in view of the convergence tests performed both by Jordan *et al.*[17] and by us. The only difference appears to be the use of a third order Hamiltonian by Jordan *et al.* in contrast to the second order approximation used by us. In this connection we would like to point out that our band-structure results agree quite well with those obtained by the entirely different interface approach to be presented in the following sections. This is true in particular for the DO_{23} structure where the expansions (1,2) are expected to be most accurate.

TABLE II. Calculated structural energy differences in mRy/A_3B of the DO_{22} and DO_{23} structures relative to $L1_2$ obtained in the present work by LMTO-ASA band-structure calculations compared to those obtained by the linear augmented plane wave (LAPW) method using Wigner exchange correlation (Ref. 16) and the LMTO calculations by Jordan *et al.* (Ref. 17).

Structure	DO_{22}			DO_{23}	
Compound	Present LMTO-ASA	LMTO-ASA[a]	LAPW[b]	Present LMTO-ASA	LMTO-ASA[a]
Cu_3Pd	4.81		2.79	0.45	
Ag_3Mg	-2.91	-0.6		-4.62	-3.1

[a]See Ref. 17.
[b]Unrelaxed values from Ref. 16.

VI. INTERFACE CALCULATIONS OF STRUCTURAL STABILITY

A. Cu_3Pd

In Fig. 3 we present the calculated separation-dependent two- and three-body interactions for Cu_3Pd in the $L1_2$ structure. It is seen that the two-body interaction, i.e., the interaction between neighboring antiphase boundaries, is highly repulsive at small separations and that it exhibits a slow decay at separations M larger than three $L1_2$ unit cells. At a separation $M = 19$ not included in the figure the two-body interaction has fallen to -0.13 mRy, and hence, it is not only long ranged but also weakly oscillating. Similar oscillations but of shorter periods are found in Cu_3Al and Ag_3Mg. It is furthermore seen that the leading three-body interaction $K_{n,m}$, where $(n,m) = (M, M-1)$, does not extend beyond $M = 3$.

The total energy per formula unit of one-dimensional long-period superstructures may be obtained by means of the calculated interactions and the expansion (1). The result for Cu_3Pd is shown in Fig. 4 as a function of the mean separation M between antiphase boundaries. The total energies for $M = 1$ and 2 correspond to the structural energies of the DO_{22} and DO_{23} structures, respectively, relative to the $L1_2$ structure, and it is therefore possible to assess the accuracy of the interface approach by direct band-structure calculations. In Table III we compare structural energies obtained by LMTO-ASA band-structure calculations using a second order Hamiltonian with those of the APB Hamiltonian and the ANNNI model. It is seen that in general the agreement between the three sets of calculations is better than 34% for the DO_{22} structure and 18% for the DO_{23} structure, which may be considered satisfactory in view of the fact that the expansions are expected to be less accurate for small separations where higher order terms may be needed.

In Fig. 4 we have included long-range superstructures of the form $\langle ii \rangle$ and $\langle i\, i-1 \rangle$ since it is only among these structures that the ground state of the expansion (1) is to be found. This is so because the two-body interaction as a function of M is highly nonlinear with a positive second derivative which discriminates against structures of the form $\langle ij \rangle$ where $i \gg j$. The figure includes also the

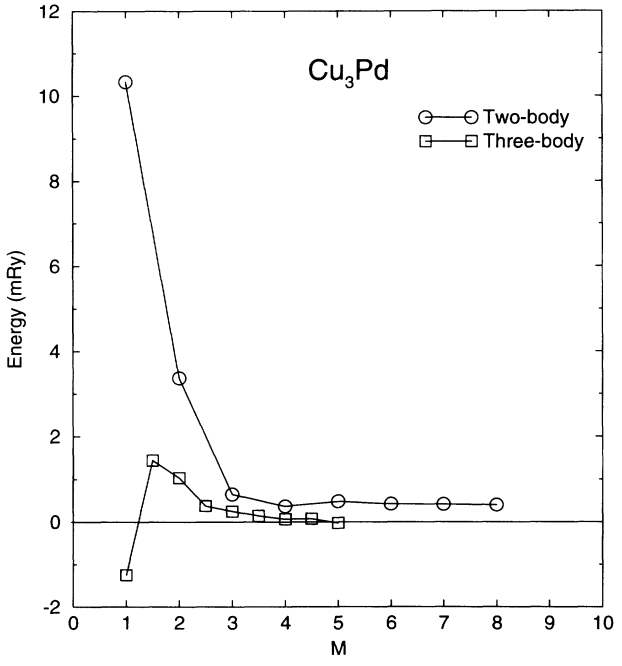

FIG. 3. Interaction energies of successive (001) APB's for Cu_3Pd in the $L1_2$ structure. Circles denote the energy of interaction for an isolated pair of (001) APB's separated by the distance M, $I(M)$. Squares show the three-body interaction term $K(M, M-1)$ for three successive APB's at distances $M-1$ and M. See text for details. Energies are in mRy/(surface cell) and distance in units of the $L1_2$ lattice spacing.

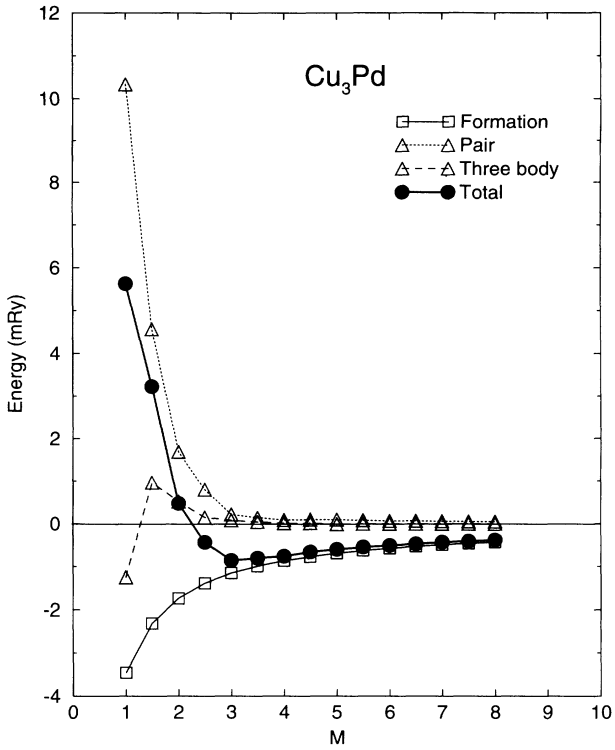

FIG. 4. Total energy of 1D-LPS's of the type $\langle i-1\, i \rangle$ in Cu_3Pd calculated from contributions of APB formation energy, pair, and three-body interactions. All energies are per Cu_3Pd.

In Fig. 4 we have included long-range superstructures of the form $\langle ii \rangle$ and $\langle i\, i-1 \rangle$ since it is only among these structures that the ground state of the expansion (1) is to be found. This is so because the two-body interaction as a function of M is highly nonlinear with a positive second derivative which discriminates against structures of the form $\langle ij \rangle$ where $i \gg j$. The figure includes also the

TABLE III. Calculated structural energy differences in mRy/A_3B of the DO_{22} and DO_{23} structures relative to $L1_2$ obtained in the present work by LMTO-ASA band-structure calculations (Band) as well as by the interface expansions (APB) and (ANNNI) described in the text.

Structure	DO_{22}			DO_{23}		
Compound	Band	APB	ANNNI	Band	APB	ANNNI
Cu_3Pd	4.81	5.53	3.96	0.45	0.48	-0.17
Cu_3Al	-2.54	-1.66	-2.09	-1.75	-1.44	-1.89
Ag_3Mg	-2.91	-1.98	-3.39	-4.62	-4.23	-4.66

individual contributions to the total energy and we may thereby arrived at the following picture of the stability of the long-period superstructures. The energy of formation of antiphase boundaries is proportional to their density and hence inversely proportional to the mean separation M. This term will therefore favor superstructures with short periods. On the other hand, the interaction between nearest-neighbor antiphase boundaries is highly repulsive at small separations, and since the three-body interaction is only a minor correction, it is the competition between formation energy and the repulsive interaction between nearest-neighbor antiphase boundaries which causes a particular one-dimensional long-period superstructure to form.

Based on the results in Fig. 4 the ground state of Cu_3Pd will be a one-dimensional superstructure with $M = 3$, i.e., of the form $\langle 3 \rangle$. However, the superstructures $\langle 34 \rangle$ and $\langle 4 \rangle$ are rather close in energy to this ground state as may be seen in Table IV, and hence they may be stable at elevated temperatures. One may note that the APB Hamiltonian and the ANNNI model give the same ground state, although it appears that the ANNNI model is less accurate for small antiphase boundary separations. The predicted ground state and also the shallowness of the minimum in the total energy are in agreement with the experimental situation where, as described in Sec. I A, depending on concentration and temperature one finds superstructures in Cu_3Pd of the forms $\langle 3 \rangle$, $\langle 4 \rangle$, and $\langle 45 \rangle$.

B. Cu_3Al

It follows from Table III that if the formation of antiphase boundaries is neglected Cu_3Al might form in the DO_{22} structure. Since the antiphase boundary energy E_{APB} listed in Table I is negative also in the DO_{22} structure one would expect Cu_3Al to form long-period superstructures based on this structure. In Fig. 5 we therefore present the calculated two- and three-body interactions for Cu_3Al in the DO_{22} structure. It is seen that the two-body interaction, i.e., the interaction between neighboring antiphase boundaries, is highly repulsive at small separations and that it exhibits an oscillatory decay with a period of oscillation of approximately 10 $L1_2$ lattice spacings at separations M' larger than 3. It is furthermore seen that the leading three-body interaction $K_{n,m}$, where $(n,m) = (M', M' - 1)$, does not extend beyond $M' = 5$.

The total energy per formula unit of one-dimensional long-period superstructures obtained by means of the calculated interactions and the expansion (1) is shown in Fig. 6. Based on these results the ground state of Cu_3Al is expected to be a one-dimensional superstructure with $M' = 5$, i.e., of the form $\langle 5 \rangle$. However, the superstructures $\langle 4 \rangle$, $\langle 45 \rangle$, and $\langle 56 \rangle$ are rather close in energy to the ground state as may be seen in Table V, and hence they may be stable at elevated temperatures. The predicted ground state and also the shallowness of the minimum in the total energy are in agreement with the experimental situation where, as described in Sec. I A, depending on concentration and temperature one finds superstructures in Cu_3Al of the forms $\langle 4 \rangle$, $\langle 45 \rangle$, and $\langle 5 \rangle$.

TABLE IV. Calculated structural energy differences in mRy/A_3B of one-dimensional long-period superstructures in Cu_3Pd relative to $L1_2$.

1D-LPS	$\langle 23 \rangle$	$\langle 3 \rangle$	$\langle 34 \rangle$	$\langle 4 \rangle$	$\langle 45 \rangle$	$\langle 5 \rangle$
APB	-0.43	-0.85	-0.80	-0.75	-0.66	-0.60
ANNNI	-0.72	-1.04	-0.93	-0.85	-0.74	-0.66

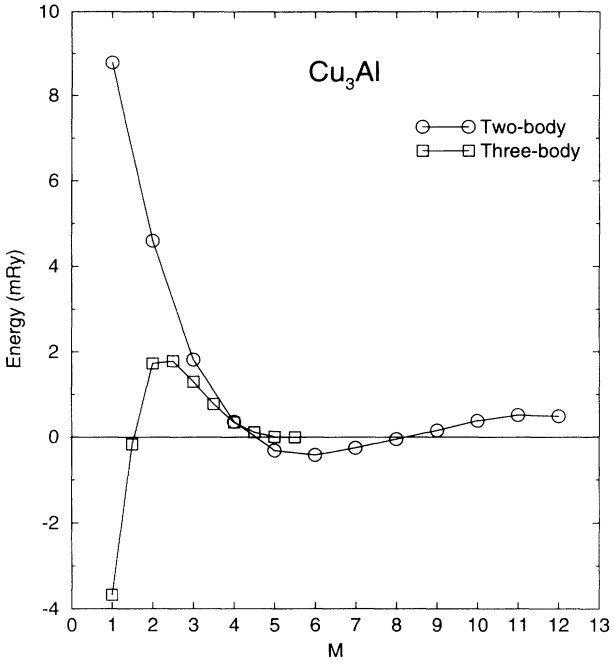

FIG. 5. Interaction energies of successive (001) APB's for Cu_3Al in the $L1_2$ structure. See Fig. 3 for notation. Energies are in mRy/(surface cell) and distance is in units of the $L1_2$ lattice spacing.

C. Ag_3Mg

The calculated two- and three-body interactions for Ag_3Mg in the $L1_2$ structure are presented in Fig. 7. In this case the two-body interaction is repulsive for small separations only at $M = 1$ and exhibits an oscillatory decay with a period of approximately 4 $L1_2$ lattice spacings. Hence, both the formation term and the two-body term drive Ag_3Mg into the DO_{23} structure as may be inferred from Fig. 8 where we show the total energy obtained by means of the calculated interactions and the expansion (1). Based on these results the ground state of Ag_3Mg is seen to be the one-dimensional superstructure with $M = 2$, i.e., the DO_{23} structure. This is in agreement with the calculations of Jordan *et al.*[17] and also with experiments in that the simplest of the observed superstructures is the DO_{23} structure.[13,14]

Jordan *et al.* related the formation of superstructures of the form $\langle 2^j 1 \rangle$ at different concentrations to the change

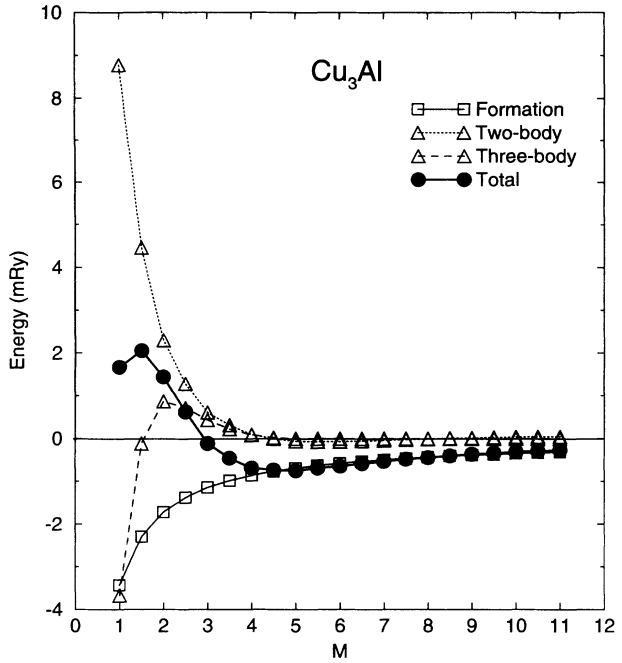

FIG. 6. Total energy of 1D-LPS's of the type $\langle i-1\,i\rangle$ in Cu_3Al calculated from contributions of APB formation energy, pair, and three-body interactions. All energies are per Cu_3Al.

of a Fermi surface dimension calculated within the rigid band model. Thereby, one may understand the variation of j observed experimentally over the concentration range 22–26 %. Here, we complement this picture by direct calculation of the total energy of the superstructures. We find that the minimum in the total energy shown in Fig. 8 and Table VI is now quite deep and will not favor superstructures of the form $\langle M-1, M\rangle$ and $\langle M, M+1\rangle$ which were close to the ground state in Cu_3Pd and Cu_3Al. Instead, superstructures with a large component of the DO_{23} structure, i.e., of the form $\langle 2^j 1\rangle$ where j is an integer, may be close in energy to the ground state as illustrated in the insert in Fig. 8.

The energy of structures of the form $\langle 2^j 1\rangle$ may be obtained as a function of j or M directly from the APB Hamiltonian. One finds

$$E_{\langle 2^j 1\rangle} = E_{\langle 2\rangle} + \frac{E_{M=1}(DO_{23})}{2j+1}\,, \tag{4}$$

where

$$E_{M=1}(DO_{23}) = \tfrac{1}{2}[E_{\mathrm{APB}}(L1_2) - I_2 - 3K_{2,2} + 2I_1 + 4K_{1,2}] \tag{5}$$

TABLE V. Calculated structural energy differences in mRy/A_3B of one-dimensional long-period superstructures in Cu_3Al relative to $L1_2$.

1D-LPS	⟨3⟩	⟨34⟩	⟨4⟩	⟨45⟩	⟨5⟩	⟨56⟩
APB	-0.11	-0.45	-0.69	-0.74	-0.75	-0.69
ANNNI	-0.49	-0.64	-0.76	-0.78	-0.79	-0.74

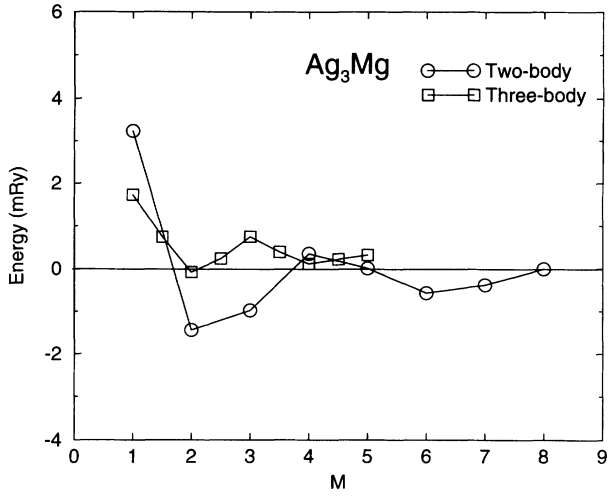

FIG. 7. Interaction energies of successive (001) APB's for Ag_3Mg in the $L1_2$ structure. See Fig. 3 for notation. Energies are in mRy/(surface cell) and distance is in units of the $L1_2$ lattice spacing.

is the energy of formation of an isolated antiphase domain of length 1 in the DO_{23} structure given in terms of the two- and three-body interactions. For Ag_3Mg the expansion (5) gives 2.1 mRy which compares favorably with the value of 1.7 mRy found by direct calculation (see Table I). In the inset in Fig. 8 we have plotted the energy of the structures $\langle 2^j 1\rangle$, $j = 1, 2, ..., 9$, calculated by (4) together with the results from the analogous ex-

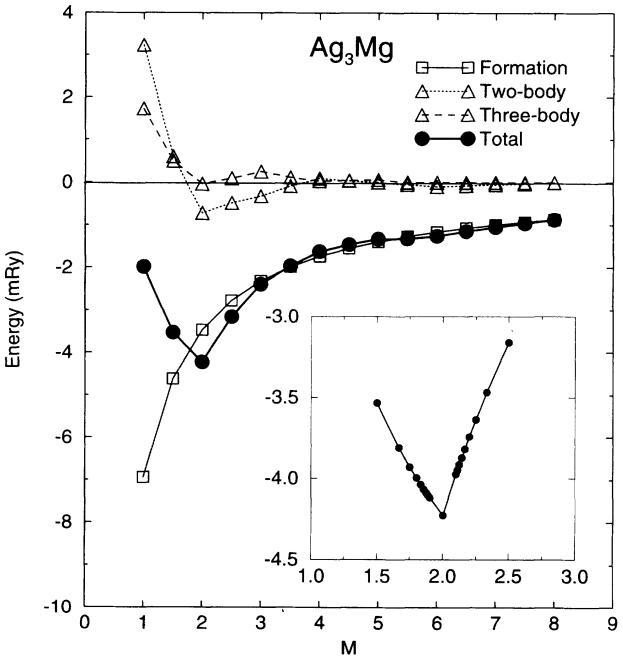

FIG. 8. Total energy of 1D-LPS's of the type $\langle i-1\,i\rangle$ in Ag_3Mg calculated from contributions of APB formation energy, pair, and three-body interactions. All energies are per Ag_3Mg. The insert shows the energy of structures of the form $\langle 2^j 1\rangle$, and $\langle 2^j 3\rangle$, $j = 1, 2, ..., 9$.

TABLE VI. Calculated structural energy differences in mRy/A_3B of one-dimensional long-period superstructures in Ag_3Mg relative to $L1_2$.

1D-LPS	DO_{22}	$\langle 12 \rangle$	DO_{23}	$\langle 23 \rangle$	$\langle 3 \rangle$
APB	-1.98	-3.53	-4.23	-3.16	-2.39
ANNNI	-3.39	-3.23	-4.66	-3.49	-2.58

TABLE VII. Interaction parameters J_n of the generalized ANNNI model, Eq. (2). Energies are in mRy/A_3B.

n	1	2	3	4	5	6	7
Cu_3Pd	2.55	-1.06	-0.61	-0.10	0.04	-0.02	0.00
Cu_3Al	-1.53	-0.35	0.33	-0.20	0.14	-0.07	0.01
Ag_3Mg	-1.49	-1.29	-0.22	0.42	0.06	-0.19	0.05

pression for the structures $\langle 2^j 3 \rangle$, $j = 1, 2, ..., 9$. It may be realized that the structures $\langle 2^j 1 \rangle$ are considerably lower in energy than the structures $\langle 2^j 3 \rangle$ for the same j. As a result one may expect these superstructures to be stable at elevated temperatures and at concentrations off stoichiometry. This is in complete agreement with the experimental situation as described in Sec. I A where one finds superstructures of the form $\langle 2^j 1 \rangle$ with j taking on values in the range from 2 to 19.

VII. MODEL HAMILTONIANS

The total energies presented in Figs. 4, 6, and 8 have been obtained by means of the calculated interactions and the APB Hamiltonian discussed in Sec. IV B. To complement these calculations we have also derived the parameters for the ANNNI Hamiltonian (2,3) and calculated the total energies within this model. The parameters are listed in Table VII and the results are presesented in Tables IV, V, and VI. It is seen in the tables that although the ANNNI model in general results in lower energies than the APB Hamiltonian both models lead to the same ground state. However, the ANNNI model fails in predicting a negative relative stability of the DO_{23} structure in Cu_3Pd (Table III), and perhaps also in predicting an incorrect asymmetry of the minimum in the total energy in Ag_3Mg (Table VI).

Since the APB and ANNNI Hamiltonians represent two apparently similar expansions of the interactions present in 1D long-period superstructures one may illustrate the connection between the two by calculating the energy of a 1D superstructure with a period of $M = 3$. We find

$$E^{\mathrm{APB}}_{\langle 3 \rangle} = \tfrac{1}{3}(E_{\mathrm{APB}} + I_3 + K_{3,3} + \cdots) \tag{6}$$

and

$$E^{\mathrm{ANNNI}}_{\langle 3 \rangle} = \tfrac{1}{3}(E_{\mathrm{APB}} + I_3 - I_6 + \cdots), \tag{7}$$

where, in a sense, the two expansions differ only in the way they are truncated. That is, if we neglect the three-body term in (6) and truncate the ANNNI expansion at a range of 5 the energy of the $M = 3$ structure would be the same in the two models. However, by construction the correction $K_{3,3}$ to the APB Hamiltonian leads to a perfect agreement with the *ab initio* results while the correction $-I_6$ to the ANNNI model is dictated by the form of the Hamiltonian and therefore may be less accurate. As a result, the expansions tend to agree for longer separations where the three-body term may be neglected but disagree for shorter periods. Inspection of Figs. 3–8 and Tables IV–VI shows that this is indeed what happens and on account of the close fit to the *ab initio* calculations one may therefore prefer the APB Hamiltonian over the ANNNI model in expansions of the total energy of long-period superstructures.

VIII. CONCLUSION

We have determined the total energy of one-dimensional long-period superstructures in Cu_3Pd, Cu_3Al, and Ag_3Mg based on an APB Hamiltonian and the calculated energy of formation of a single antiphase boundary and the two- and three-body interactions viewed as functions of the antiphase boundary separation. Thereby, we arrive at a picture in which the long-period superstructures are formed as the result of the competition between the energy gained by forming antiphase boundaries and the repulsive interaction of nearest-neighbor antiphase boundaries. The calculated ground states are in agreement with experiments and also with the previous calculation by Jordan *et al.*[17] of the formation of superstructures in Ag_3Mg. Finally, we provide the parameters for the ANNNI Hamiltonian which may also be used to study the structural phase transitions in the three compounds considered here.

ACKNOWLEDGMENTS

The work of N.M.R. was supported by grants from the Danish Natural Science Foundation (SNF) and the Danish Technical Science Foundation (STVF). Center for Atomic-Scale Materials Physics is sponsored by the Danish National Research Foundation. Part of the work was supported by grants from the Novo Nordisk Foundation and the Danish research councils through the Danish Center for Surface Reactivity.

[1] K. Schubert, M. Wilkens, and R. Haufler, Z. Metallkd. **46**, 692 (1955).
[2] D. Watanabe, M. Hirabayashi, and S. Ogawa, Acta Crystallogr. **8**, 510 (1955).
[3] D. Broddin, G. Van Tendeloo, J. Van Landuyt, S. Amelinckx, R. Portier, M. Guymont, and A. Loiseau, Philos. Mag. A **54**, 395 (1986).
[4] S. Takeda, J. Kulik, and D. de Fontaine, J. Phys. F **18**, 1387 (1988).
[5] E. Bernard and P. Duval, Phys. Status Solidi A **34**, 135 (1976).
[6] N. Kuwano, T. Doi, and T. Eguchi, Trans. Jpn. Inst. Met. **18**, 807 (1977).
[7] N. Kuwano, H. Mishio, and T. Eguchi, in *Proceedings of the International Conference on Modulated Structures,* Kailua Kona, Hawaii, 1979, edited by J. M. Cowley, M. B. Salamon, and B.J. Wuensch, AIP Conf. Proc. No. 53 (AIP, New York, 1979), p. 273.
[8] D. Broddin, G. Van Tendeloo, J. Van Landuyt, S. Amelinckx, and M. De Graef, Philos. Mag. A **59**, 979 (1989).
[9] K. Schubert, B. Kiefer, M. Wilkens, and R. Haufler, Z. Metallkd. **46**, 692 (1955).
[10] K. Fujiwara, M. Hirabayashi, D. Watanabe, and S. Ogawa, J. Phys. Soc. Jpn. **13**, 167 (1958).
[11] K. Hähnis, J. Mäki, and P. Paalassalo, Acta Metall. **19**, 15 (1971).
[12] R. Portier, D. Gratias, M. Guymont, and W.M. Stobbs, Acta Metall. A **36**, 190 (1980); M. Guymont, R. Portier, D. Gratias, and W.M. Stobbs, in *Proceedings of the International Conference on Modulated Structures* (Ref. 7), p. 256.
[13] J. Kulik, S. Takeda, and D. de Fontaine, Acta Metall. **35**, 1137 (1987).
[14] Y. Fujino, H. Sato, and N. Otsuka, in *Materials Problem Solving with the Transmission Electron Microscope,* edited by L.W. Hobbs, K.H. Westmacott, and D.B. Williams, MRS Symposia Proceedings No. 62 (Materials Research Society, Pittsburgh, 1986), p. 349.
[15] Y. Fujino, Phys. Rev. B **42**, 5373 (1990).
[16] Z.W. Lu, S.-H. Wei, A. Zunger, S. Frota-Pesso, and L.G. Ferreira, Phys. Rev. B **44**, 512 (1991).
[17] R.G. Jordan, Y. Liu, S.L. Qiu, X. Xu, P.J. Durham, and G.Y. Guo, Phys. Rev. B **47**, 16 521 (1993).
[18] N.M. Rosengaard and H.L. Skriver (unpublished).
[19] H.L. Skriver and N.M. Rosengaard, Phys. Rev. B **43**, 9538 (1991).
[20] N.M. Rosengaard and H.L. Skriver, Phys. Rev. B **47**, 12 865 (1993).
[21] H. Sato and R.S. Toth, Phys. Rev. **127**, 469 (1962).
[22] B.L. Györffy, A. Barbieri, D.D. Johnson, D.M. Nicholson, W.A. Shelton, and G.M. Stocks, in *Alloy Phase-Stability and Design,* edited by G.M. Stocks, D.P. Pope, and A.F. Giemi, MRS Symposia Proceedings No. 186, Materials Research Society, Pittsburgh, 1991), p. 65.
[23] B.L. Györffy and G.M. Stocks, Phys. Rev. Lett. **50**, 374 (1983).
[24] G. Ceder, D. de Fontaine, H. Dreysse, D.M. Nicholson, G.M. Stocks, and B.L. Györffy, Acta Metall. **38**, 2209 (1990).
[25] G. Ceder, P. Huang, S. Menon, D. de Fontaine, D.M. Nicholson, G.M. Stocks, and B.L. Györffy, in *Alloy Phase Stability and Design* (Ref. 22), p. 65.
[26] M.E. Fisher and W. Selke, Phys. Rev. Lett. **44**, 1502 (1980).
[27] D. de Fontaine and J. Kulik, Acta Metall. **33**, 145 (1985).
[28] W. Selke, in *Alloy Phase Stability,* Vol. 106 of *NATO Advanced Study Institute, Series E: Applied Sciences*, edited by G.M. Stocks and A. Gonis (Kluwer, Dordrecht, 1989), p. 205.
[29] G. Ceder, M. De Graef, L. Delaey, J. Kulik, and D. de Fontaine, Phys. Rev. B **39**, 381 (1989).
[30] K. Oshshima and J. Harada, in *Modulated Structures* (Ref. 7), p. 289.
[31] O.K. Andersen, Phys. Rev. B **12**, 3060 (1975).
[32] O. Gunnarsson, O. Jepsen, and O.K. Andersen, Phys. Rev. B **27**, 7144 (1983).
[33] H.L. Skriver, *The LMTO Method* (Springer-Verlag, Berlin, 1984).
[34] O.K. Andersen and O. Jepsen, Phys. Rev. Lett. **53**, 2571 (1984).
[35] O.K. Andersen, O. Jepsen, and D. Glötzel, in *Highlights of Condensed-Matter Theory*, edited by F. Bassani, F. Fumi, and M. P. Tosi (North-Holland, New York, 1985).
[36] O.K. Andersen, Z. Pawlowska, and O. Jepsen, Phys. Rev. B **34**, 5253 (1986).
[37] W.R.L. Lambrecht and O.K. Andersen, Surf. Sci. **178**, 256 (1986); (private communication).
[38] J. Kudrnovsky, P. Weinberger, and V. Drchal, Phys. Rev. B **44**, 6410 (1991).
[39] O.K. Andersen (unpublished).
[40] S.L. Cunningham, Phys. Rev. B **10**, 4988 (1974).
[41] D.M. Ceperley and B.J. Alder, Phys. Rev. Lett. **45**, 566 (1980).
[42] J. Perdew and A. Zunger, Phys. Rev. B **23**, 5048 (1981).
[43] P. Bak and R. Bruinsma, Phys. Rev. Lett. **49**, 249 (1982).
[44] W.B. Pearson, *Handbook of Lattice Spacings and Structures of Metals* (Pergamon, New York, 1958), Vol. 1; *ibid.* (Pergamon, New York, 1967), Vol. 2.